INFECTION AND IMMUNITY, Nov. 1996, p. 4463–4471 Vol. 64, No. 11
0019-9567/96/$04.00+0

Identification, Characterization, and Expression of the BiP Endoplasmic Reticulum Resident Chaperonins in *Pneumocystis carinii*

TIMOTHY T. STEDMAN† AND GREGORY A. BUCK*

Department of Microbiology and Immunology, Medical College of Virginia Campus, Virginia Commonwealth University, Richmond, Virginia 23298-0678

Received 17 April 1996/Returned for modification 18 June 1996/Accepted 2 August 1996

We have isolated, characterized, and examined the expression of the genes encoding BiP endoplasmic reticulum (ER) resident chaperonins responsible for transport, maturation, and proper folding of membrane and secreted proteins from two divergent strains of *Pneumocystis carinii*. The BiP genes, *Pcbip* and *Prbip*, from the *P. c. carinii* (prototype) strain and the *P. c. rattus* (variant) strain, respectively, are single-copy genes that reside on chromosomes of ~330 and ~350 kbp. Both genes encode ~72.5-kDa proteins that are most homologous to BiP genes from other organisms and exhibit the amino-terminal signal peptides and carboxyl-terminal ER retention sequences that are hallmarks of BiP proteins. We established short-term *P. carinii* cultures to examine expression and induction of *Pcbip* in response to heat shock, glucose starvation, inhibition of protein transport or N-linked glycosylation, and other conditions known to affect proper transport, glycosylation, and maturation of membrane and secreted proteins. These studies indicated that *Pcbip* mRNA is constitutively expressed but induced under conditions known to induce BiP expression in other organisms. In contrast to mammalian BiP genes but like other fungal BiP genes, *P. carinii* BiP mRNA levels are induced by heat shock. Finally, the *Prbip* and *Pcbip* coding sequences surprisingly exhibit only ~83% DNA and ~90% amino acid sequence identity and show only limited conservation in noncoding flanking and intron sequences. Analyses of the *P. carinii* BiP gene sequences support inclusion of *P. carinii* among the fungi but suggest a large divergence and possible speciation among *P. carinii* strains infecting a given host.

Pneumocystis carinii is an important opportunistic pathogen of immunocompromised patients and infects up to 80% of patients with AIDS (2). Relatively little is known of the basic biology of this organism, largely because of its relatively recent ascendance to the status of an important opportunistic pathogen but also because of the lack of long-term continuous culture systems. The cell surface composition of this lung pathogen has been examined in some detail (11, 12, 40, 62), major antigens have been characterized (25, 29, 58), and ultrastructural analyses have identified most of the prototype eukaryotic organelles in each of the two basic life cycle stages of *P. carinii*. Although these surface antigens are clearly critical in all interactions between the pathogen and the host, the mechanisms by which they are transported, processed, and matured have not been studied. The phylogenetic placement of *P. carinii* among the fungi was recently confirmed by analyses of several rRNA, mitochondrial, and structural protein coding genes, although this classification remains somewhat controversial (14, 15, 19, 54, 60). Finally, recent reports have suggested that *P. carinii* strains have restricted host ranges but that multiple strains may infect a given host (3, 50, 52, 55). Two distinct isoforms, prototype and variant, have been identified in rats (10), and multiple karyotype variants of the prototype isoform have been reported (9). A proposed revision in the taxonomic nomenclature designates the prototype and variant isoforms as *P. c. carinii* and *P. c. rattus*, respectively (53).

Members of the ubiquitous HSP70 family of proteins play crucial roles in controlling protein folding and trafficking (reviewed in reference 21) and are among the most highly conserved proteins known (23, 26). The HSP70 gene family diverged into different functional classes of molecular chaperones early in the evolution of eukaryotes (4). The HSP70 homolog BiP is an essential resident protein of the endoplasmic reticulum (ER) and plays an important role in the folding and assembly of immature proteins within the ER lumen (6). BiP, also known as grp78, is a 72- to 78-kDa glucose-regulated protein that constitutes 5 to 10% of the lumenal protein (21). BiP binds transiently to nascent, incompletely folded proteins destined for secretion, proteins involved in the secretory pathway, and transmembrane proteins prior to N-linked glycosylation or folding in the ER. The principal role of BiP appears to be the stabilization of nascent chains in a folding-competent state and preventing formation of protein aggregates (reviewed in reference 24), although BiP also appears to aid translocation of nascent chains into the ER.

Herein, we characterize BiP genes from the prototype and variant strains of rat *P. carinii*. We report the genomic and cDNA sequences for *P. c. carinii* BiP (*Pcbip*) and the genomic sequence for *P. c. rattus* BiP (*Prbip*). The hallmark leader peptide and ER retention signal sequences of BiP proteins are identified in the inferred protein sequence. We use short-term *P. carinii* cultures to show that, as in other organisms, *Pcbip* expression is probably constitutively expressed but induced in response to heat shock, glucose starvation, and other conditions known to affect protein transport and maturation. DNA elements that may be responsible for this regulation were identified in sequences upstream from the *Pcbip* coding sequence.

* Corresponding author. Mailing address: Department of Microbiology and Immunology, Box 980678, Medical College of Virginia Campus, Virginia Commonwealth University, Richmond, VA 23298-0678. Phone: (804) 828-2318. Fax: (804) 828-9946. Electronic mail address: buck@gems.vcu.edu.

† Present address: Section of Infectious Diseases, Department of Internal Medicine, Yale University School of Medicine, New Haven, CT 06520-8022.

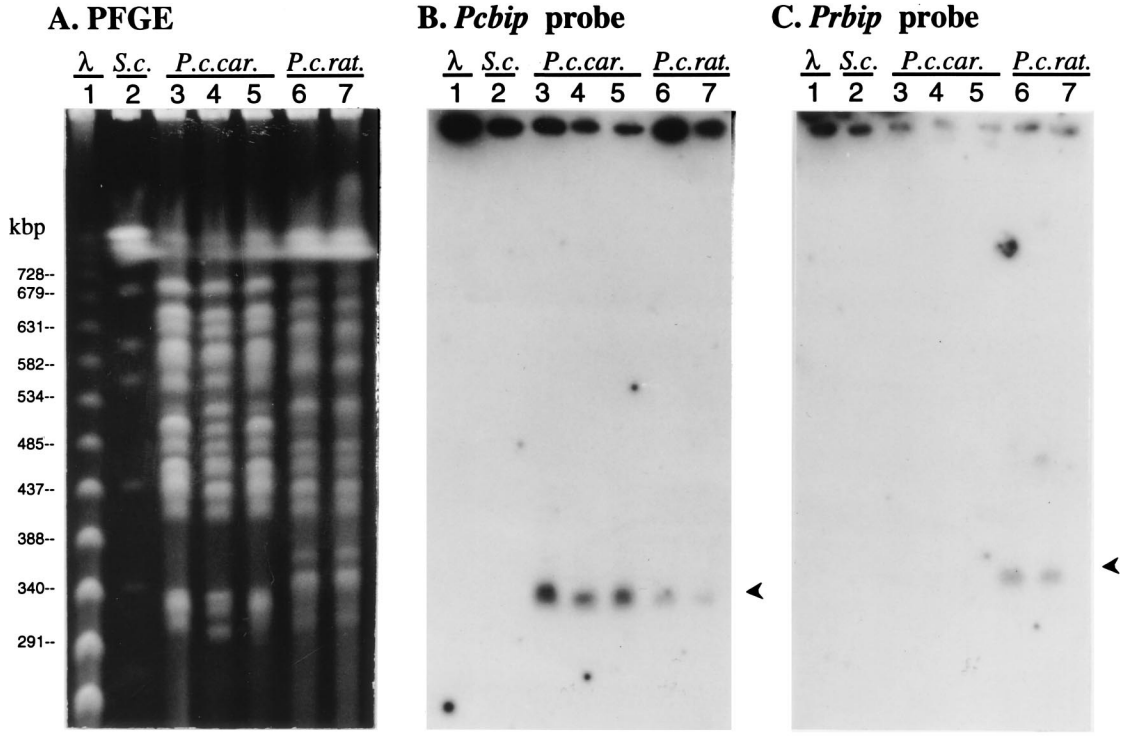

FIG. 1. Karyotype analysis of *Pcbip* and *Prbip* genes from *P. c. carinii* prototype and *P. c. rattus* variant strains. (A) CHEF gel of *P. carinii* chromosomes. Lanes: 1, bacteriophage λ concatemer molecular size standards; 2, *S. cerevisiae* chromosome standards; 3 to 5, *P. c. carinii* prototype strain, isolates 101393, 102093, and 101193, respectively; 6 and 7, natural coinfections of *P. c. rattus* variant strain (predominant) and *P. c. carinii* prototype strain, isolates 319931 and 319932, respectively. The approximate sizes of the λ markers are indicated. (B) Southern blot analysis of gel shown in panel A using *Pcbip* gene-specific oligonucleotide probe p380Ar 5′ end-labeled as described in Materials and Methods. The probe hybridized strongly to a ~330-kbp chromosome (arrowhead) in the *P. c. carinii* prototype isolates (lanes 3 to 5) but only weakly to the ~330-kbp chromosome in the *P. c. rattus* variant isolates coinfected with a minority of *P. c. carinii* (lanes 6 and 7). (C) Southern blot analysis using a *Prbip* gene-specific oligonucleotide probe p380Br 5′ end-labeled as described in Materials and Methods. The probe hybridized to a ~355-kbp *P. c. rattus* variant strain chromosome (arrowhead) but not to the ~330-kbp *P. c. carinii* prototype strain chromosome (lanes 6 and 7).

Finally, phylogenetic analysis by parsimony- and distance matrix-based methods supported classification of *P. carinii* among the fungi, although the BiP genes of the prototype and variant isoforms show a surprising divergence, suggesting possible speciation among *P. carinii* isolates from a given host.

MATERIALS AND METHODS

***P. carinii* isolation.** *P. carinii* was isolated from the lungs of infected Sprague-Dawley rats (Charles River, Raleigh, N.C.) immunosuppressed by twice-weekly subcutaneous injection of 25 mg of cortisone acetate (Cortone Acetate; Merck, Sharpe, & Dohme) essentially as described previously (64). Samples showing bacterial contamination, as determined by Gram staining, were discarded.

PFGE. One-tenth (~50 μl) of the intact cell pellet suspension from each *P. carinii* preparation was reserved for pulsed-field gel electrophoresis (PFGE) performed essentially as described previously (64). The chromosome-bearing agarose blocks were electrophoresed in a 1% SeaKem GTG LE agarose gel (FMC) by using a contour-clamped homogeneous electric field (CHEF) DR-II apparatus (Bio-Rad) at 14°C and 6 V/cm for 40 h with a 20- to 60-s ramp.

Nucleic acid isolation and library construction. Genomic DNA and total RNA were isolated from fresh *P. carinii* cell pellets as described previously (64) by standard protocols (48). For library construction, DNA was extracted from *P. carinii* isolate 319931, derived from a single rat naturally coinfected with both the prototype and variant strains as determined by PFGE karyotype analysis. The DNA was partially digested with *Sau*3AI and phosphatase treated by established protocols (48). Digests containing DNA fragments with an average size of 17 to 20 kbp were cloned into *Bam*HI-digested λ-DASH (Stratagene) as suggested by the manufacturer. A preamplified titer of 2.5×10^5 indicated ~50-fold coverage of the $\sim 10^7$-bp *P. carinii* genome, assuming an average insert size of 17 to 20 kbp and minimal contamination with host DNA. The library was screened with probes as described in Results and Discussion, and positive clones were plaque purified and rescreened by established techniques (48).

Oligonucleotide primer and probe design. Degenerate oligonucleotide primers were selected to target phylogenetically conserved domains of HSP70 proteins by a previously described strategy (41). PCR primers were designed with *Eco*RI and *Bam*HI sites in their 5′ ends to facilitate cloning, with an A+T codon bias in accordance with the known G+C content of rat *P. carinii* (18). The PCR primers and their sequences are as follows: HSP9, 5′-GTT GGA TCC AT(AT) GC(AT) AAT GAT CAA GG(AT) AAT-3′; HSP8, 5′-CGC GGA TCC GG(AT) GG(AT) GG(AT) AC(AT) TTT GAT GT-3′; HSP6f, 5′-GG(AT) GGA TCC AC(AT) AGA ATT CC(AT) AAA-3′; HSP6r, 5′-(AT)GG AAT TCT (AT)GT AGA(AT) CC(AT) CC(AT) AC(AT) A-3′; HSP4, 5′-CGG AAT TCC (AT)CG (AT)GG (AT)GC (AT)GG (AT)GG (AT)AT (AT)CC-3′. The sequences of *Pcbip* gene-specific oligonucleotide hybridization probes are as follows: p154Ar, 5′-TTG GTA GCT TGC CGT TGT GC-3′; p380Ar, 5′-GTG ATA AAA TTC CAC CTT GT-3′. The sequences of the *Prbip* gene-specific probes are as follows: p154Br, 5′-TTA GTA GCC TGA CGC TGA GC-3′; p380Br, 5′-GAG ATA AAA TCC CAG CCT GA-3′. The sequence of the *P. carinii* actin probe (PcAct) was based on the published sequence (19), namely, 5′-GAA GCT GTA TGA ATT TCT TGT TCA-3′. Primers used for rapid amplification of cDNA ends (RACE)-PCR included the RACE anchor (5′-CTC GCT CGC CCA GGI GGI GGI GGI GGI GGI GG-3′) and a *Pcbip*-specific primer, RACE154 (5′-CTG GTT CGG CCC ATT GGT AGC TTG CCG TTG TGC-3′). Each of these latter primers have 5′ termini required for ligation into the pDirect cloning vector (Clontech). All oligonucleotides were synthesized in the MCV-VCU DNA Core Laboratory. Oligonucleotides used as hybridization probes were confirmed by Northern (RNA) and Southern analyses to be specific for *P. carinii*, and not host, nucleic acids (data not shown).

PCR amplification. PCR buffer II (Roche) was supplemented with 1.5 mM $MgCl_2$, 70 μM each deoxynucleoside triphosphate, 1 pmol of oligonucleotide primer per μl, 10 ng of DNA template per μl, and 0.025 U of *Taq* DNA polymerase (Roche) per μl in a final reaction volume of 50 to 100 μl. PCRs were performed in a Perkin-Elmer 9600 thermal cycler (Roche). Thermal cycling conditions were as follows: 94°C for 45 s, T_m − 5°C for 1 min, and 72°C for 1 min, for 35 rounds of amplification (the T_m is the melting temperature of the least-stable oligonucleotide primer). Reverse transcriptase PCR (RT-PCR) was performed with Tth DNA polymerase (Roche), gene-specific oligonucleotide primer sets at the concentrations described above, and total *P. carinii* RNA as described in the manufacturer's recommendations. Reverse transcription was performed at T_m − 5°C for the antisense oligonucleotide, followed by 25 rounds of PCR cycling at 95°C for 10 s, T_m − 5°C for 15 s, and 60°C for 15 s. For 5′ RACE-PCR,

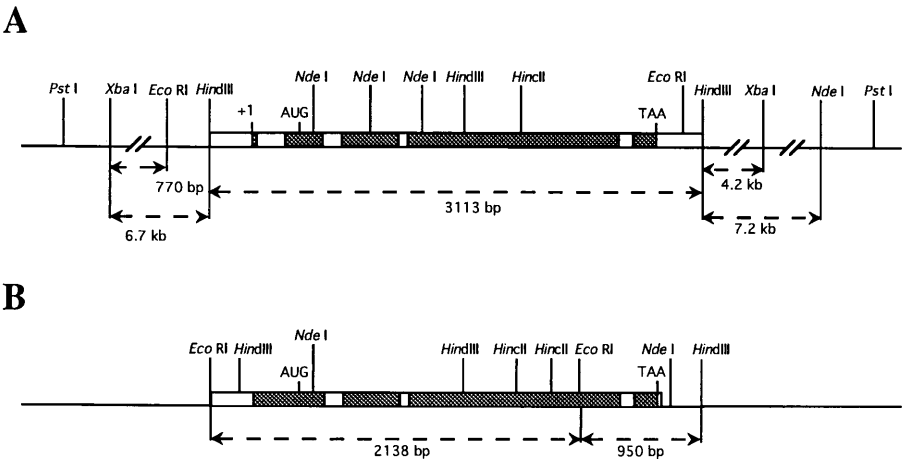

FIG. 2. Genomic context of *Pcbip* and *Prbip*. The genomic contexts of the BiP genes in *P. c. carinii* (A) and *P. c. rattus* (B) were characterized by Southern analysis using various oligonucleotides and PCR products as probes (data not shown). Boxed regions indicate the extent of the known DNA sequence. Shaded regions represent exons, with the relative positions of the transcription start point (+1), translation initiation (AUG), and termination (TAA) codons indicated. Unshaded boxed regions represent introns and the 5′ or 3′ untranscribed regions of the genes. Selected restriction sites are indicated, as are the approximate sizes of the restriction fragments. The exact localizations of the *Pst*I restriction sites flanking *Pcbip* are not known. The regions between the *Hin*dIII sites flanking *Pcbip* and the *Hin*dIII and *Eco*RI sites flanking *Prbip* are drawn to scale.

the cDNA template was synthesized from total *P. carinii* prototype strain RNA by using Superscript II RT (Life Technologies) with *Pcbip* gene-specific antisense oligonucleotides. The cDNA products were purified with Glass-Max columns (Life Technologies) and poly(dC)-tailed by using terminal deoxynucleotide transferase (New England Biolabs) and 2.5 mM dCTP. PCRs were performed with *Taq* DNA polymerase (Roche) as described above with the RACE anchor primer and the *Pcbip* gene-specific primer RACE 154. Where not indicated, the buffers used were those recommended by the enzyme manufacturers.

Purification, cloning, and sequencing of PCR products. Specific PCR products were electrophoresed in 2% NuSieve GTG agarose (FMC), excised, and phenol extracted. The purified DNA was digested with *Eco*RI and *Bam*HI and ligated into *Eco*RI-*Bam*HI-linearized pUC19. All clones were verified by sequence analysis.

Southern and Northern blot analysis. Southern blots of CHEF gels were generated as described previously (64). Prehybridization and hybridization of the blots were performed in 5 to 10 ml of Church and Gilbert (8) high-stringency buffer for PCR fragment probes or low-stringency buffer for oligonucleotide probes, at $T_m - 5°C$ for each oligonucleotide used. Hybridization probes were either purified PCR products randomly labeled with [α-^{32}P]dCTP to $>10^7$ cpm/μg with the OligoLabeling Kit (Pharmacia) or oligonucleotides 5′ end-labeled with [γ-^{32}P]ATP and T4 polynucleotide kinase (New England BioLabs) to $>5 \times 10^8$ cpm/μg. Hybridizations were performed by standard protocols (48), and the blots were washed four times for 25 min each in 2× SSC (1× SSC is 0.15 M NaCl plus 0.015 M sodium citrate)–0.5% sodium dodecyl sulfate at the hybridization temperature. Northern blots of *P. carinii* total RNA were generated essentially as described previously (48) and hybridized with labeled *P. carinii*-specific antisense oligonucleotide probes as described above. Hybridization signals were quantified on a BetaScope radioanalytic imager (Betagen).

Short-term culture and induction of the *P. carinii* BiP transcript. *P. c. carinii*-infected lungs were homogenized in low-glucose Dulbecco modified Eagle medium (Life Technologies) with 10% fetal calf serum (Life Technologies) or RPMI 1640 (Life Technologies) supplemented with 2% fetal calf serum. Lung homogenates were strained through a sterile 60-mesh wire tissue sieve (VWR). The cell suspensions were diluted to an optical density at 600 nm of ~1.5, divided into 6-ml aliquots, and incubated at the control temperature (29 or 35°C) for 3 h prior to heat shock or treatment with reagents as described in Results and Discussion. After treatment, the cells were pelleted at 13,000 × *g* for 15 s, the supernatant was decanted, and the pellets were flash-frozen in dry ice-ethanol and stored at −70°C. *P. c. carinii* (prototype) strain identity was confirmed by PFGE karyotype analysis (see below).

Phylogenetic analysis. Sequence alignments were generated by use of the Pileup and Lineup programs of the Genetics Computer Group (University of Wisconsin; GCG) Sequence Analysis package and manually optimized. Phylogenetic analysis was performed with the programs PROTPARS, DNADIST, SEQBOOT, NEIGHBOR, FITCH, and CONSENSE of the PHYLIP version 3.5c package (17). Gaps in the alignments were given a single score of 3 for each unique gap length in the parsimony analysis and were left unscored for distance matrix analysis.

Nucleotide sequence accession numbers. The sequences of *Pcbip* and *Prbip* have been deposited in GenBank under the accession numbers L46790 and U40994, respectively.

RESULTS AND DISCUSSION

Cloning of HSP70 homolog genes from prototype and variant rat *P. carinii*. Degenerate oligonucleotide primer pairs (HSP9-HSP6r, HSP8-HSP4, HSP6f-HSP4), targeted to distinct conserved domains of HSP70 genes, were used to amplify these domains from a prototype strain of rat-derived *P. carinii* as described in Materials and Methods. PCR amplification of *P. carinii* DNA with these primer pairs yielded products of the predicted size, whereas control PCR amplifications of rat liver DNA with the same primers produced no visible products (data not shown). Three specific PCR products were ligated into pUC19, sequenced, and found to encode 1,173 bp of overlapping DNA sequence with two discontinuous open reading frames exhibiting homology to eukaryotic HSP70 genes.

To verify the *P. carinii* origin of the PCR products, the cloned inserts from these plasmids were used as probes on Southern blots of CHEF gels containing *P. c. carinii* chromosomes (Fig. 1). *P. carinii* strains used for PCRs contained 17 chromosomes in a pattern similar to that described by Cushion et al. (9) for *P. c. carinii* (prototype strain) form 1, except that we observed an additional chromosome of ~555 kbp and consider chromosomes at ~450 and 430 kbp to be doublets (Fig. 1A, lanes 3 to 5). All three probes hybridized to a single 330-kbp *P. c. carinii* chromosome (data not shown, but see Fig. 1B, lanes 3 to 5). No hybridization to yeast or rat DNA controls was observed (data not shown), confirming the origin of the amplified DNA to be *P. carinii*, and not host, DNA.

A genomic library was generated in λ-DASH and screened with the cloned HSP70-specific PCR fragments as hybridization probes. The *P. carinii* used for generation of the genomic library was from isolate 319931 (Fig. 1A, lane 6), which, along with isolate 319932 (lane 7), displayed a complex CHEF karyotype indicating that these isolates were from natural coinfections of a single rat host with predominantly the *P. c. rattus* variant strain and a minor component of the *P. c. carinii* prototype strain as defined by Cushion et al. (9, 10). Two sets of

A

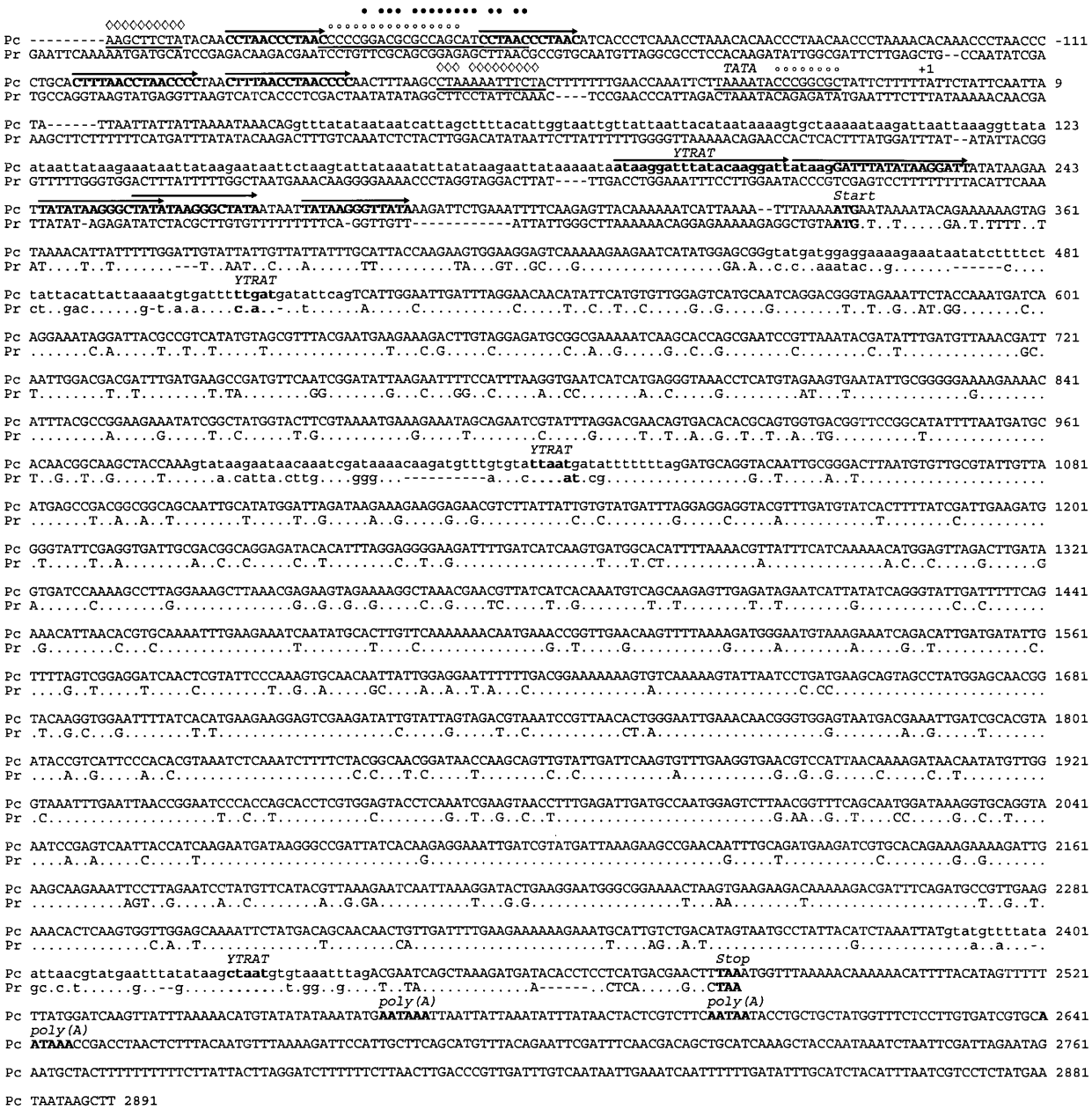

B

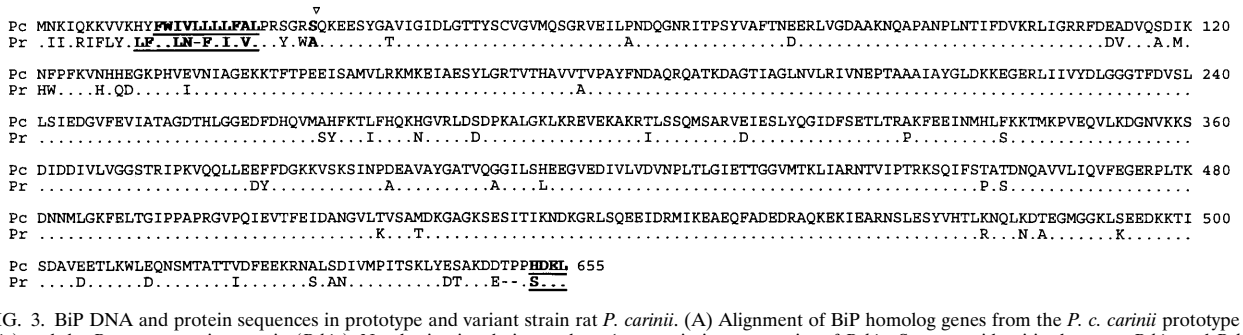

FIG. 3. BiP DNA and protein sequences in prototype and variant strain rat *P. carinii*. (A) Alignment of BiP homolog genes from the *P. c. carinii* prototype strain (*Pcbip*) and the *P. c. rattus* variant strain (*Prbip*). Numbering is relative to the +1 transcription start point of *Pcbip*. Sequence identities between *Prbip* and *Pcbip* are shown as periods and gaps are indicated with hyphens in the *Prbip* sequence. As a result of poor homology, alignment of the 5′ untranslated regions of these sequences was not possible and identities in this region are not indicated. Translation start (ATG) and stop (TAA) codons and putative polyadenylation signal sequences (AATAAA) are indicated in bold. Introns are shown in lowercase letters, and putative branch point consensus sequences of YTRAT (Y = pyrimidine and R = purine) are indicated. Potential promoter elements (GC-rich sequences, HSEs, and UPRs) in *Pcbip* are underlined, with conserved residues indicated by the following symbols:

clones were isolated and shown to bear HSP70-related genes that displayed similar but distinct restriction patterns (Fig. 2) and DNA sequences (Fig. 3). These two sets of genomic clones may have been derived from prototype and variant strains of *P. carinii*. This hypothesis was confirmed by hybridization of gene-specific probes to PFGE blots of chromosomes from the *P. carinii* isolate used for generation of the library and from known *P. c. carinii* prototype strain isolates (Fig. 1B and C). Oligonucleotide probes specific for one of the cloned HSP70 homologs hybridized strongly to a 330-kbp chromosome in the prototype isolates (Fig. 1B, lanes 3 to 5) and weakly to a ~330-kbp chromosome observed in the prototype strain (lanes 6 and 7). In contrast, probes p380Br and p154Br, specific for the second HSP70 homolog, hybridized only to a ~355-kbp chromosome present in the variant strain (Fig. 1C) but absent in the prototype strain. Finally, hybridization profiles of these gene-specific probes on Southern blots of restriction enzyme-digested genomic DNA from either the prototype or variant *P. carinii* were consistent with single-copy genes (data not shown). Thus, we concluded that we had cloned related HSP70 homologs from both prototype and variant strain *P. carinii.*

The cloned *P. carinii* HSP70 homologs are BiP genes. The sequences of the genes from the two *P. carinii* strains both exhibited four discontinuous open reading frames with homology to HSP70 and were interrupted by at least three introns (Fig. 2 and 3). The three introns and corresponding splice sites were confirmed by RT-PCR of total *P. carinii* RNA by using gene-specific primers and sequencing of the products (data not shown), and the 5′ end of the mRNA from the prototype *P. c. carinii* strain was cloned by RACE-PCR as described in Materials and Methods. The sequence of this clone identified the transcription start point (+1) and a fourth intron in the 5′ untranslated leader of the gene from this strain. We have been unable to identify the transcription start point (+1) of the mRNA of the gene from the variant *P. c. rattus* strain because of a lack of RNA. However, both of the *P. carinii* HSP70 homologs apparently consist of five exons and four introns and encode proteins of ~72.5 kDa from a translation initiation codon in exon 2. Northern analysis of *P. c. carinii* RNA showed a major transcript of ~2.5 kb (see below), consistent with the use of any of three potential poly(A) addition sequences 78, 156, and 252 bp downstream from the stop codon (Fig. 3), and a poly(A) tail length of 100 to 300 residues.

The HSP70 family includes molecular chaperones which function in protein folding and trafficking in various cellular compartments. Orthologous functional classes of these proteins evolve at similar rates in different organisms and are distinguishable from their paralogous counterparts, which arose by gene duplication and evolve independently by a low but unequal rate of evolutionary divergence in individual domains throughout the highly conserved sequences in each HSP70 class (26). Thus, to identify the function of the cloned *P. carinii* HSP70 homologs, we performed pairwise comparisons of their protein sequences with the sequences of HSP70 homologs with known function in other organisms. This analysis showed that the *P. carinii* homologs were more similar to known BiP ER resident HSP70s than to any other HSP70 family members (data not shown). Moreover, two sequence motifs exclusive to BiP HSP70 members are prominent in the proteins encoded by the HSP70-related genes isolated from the two *P. carinii* strains (Fig. 3B), namely, (i) a hydrophobic amino-terminal signal peptide and cleavage site required for targeting and translocation of BiP into the ER (6, 24) and (ii) a carboxyl-terminal signal sequence, XDEL, required for recycling BiP to the ER lumen (32, 37). The ER retention signal, HDEL, encoded by the prototype *P. c. carinii* clone is identical to that found in the yeasts *Saccharomyces cerevisiae* (39, 46) and *Kluyveromyces lactis* (49). The SDEL ER retention signal of the *P. c. rattus* HSP70-related protein is identical to that observed in *Plasmodium falciparum* BiP. Thus, we conclude that the cloned HSP70-related genes, *Pcbip* and *Prbip*, encode BiP homologs PcBiP and PrBiP from the prototype and variant strains *P. c. carinii* and *P. c. rattus*, respectively.

Expression and stress induction of *Pcbip*. BiP genes in other organisms are expressed constitutively, but BiP mRNA levels are induced by conditions that cause an accumulation of unfolded or immature proteins in the ER, e.g., heat shock, glucose starvation mediated by α-deoxyglucose treatment, inhibition of N-linked glycosylation with tunicamycin, inhibition of export from the ER with brefeldin A, or perturbation of intracellular calcium levels by agents including the ER-specific Ca^{2+} ATPase inhibitor thapsigargin or the calcium ionophore A23187 (30, 31, 34, 43, 57). These treatments induce BiP mRNA levels in *S. cerevisiae* (39, 46, 57), *Schizosaccharomyces pombe* (42), and mammalian cells (31, 34, 43, 45), although mammalian BiP genes are not significantly induced by heat shock (61). We examined the *P. carinii* BiP mRNA levels in response to treatment with these agents in short-term in vitro cultures as described in Materials and Methods. Preincubations were either at 29°C to parallel analyses of BiP expression in *S. cerevisiae* and other fungi (42) or at 35°C to approximate temperatures within a host lung. *Pcbip* expression was measured by Northern hybridization of RNA isolated from short-term cultures of prototype *P. carinii* after treatment with the various agents (Fig. 4). Specific mRNA levels were compared with BiP mRNA levels in untreated cultures normalized to the ~1.4-kb *P. carinii* actin mRNA control detected with the *P. carinii* actin-specific probe PcAct (Table 1).

Pcbip mRNA was detected under all conditions examined, suggesting that as for other organisms, expression of BiP in *P. carinii* is constitutive. However, the levels of *Pcbip* mRNA were clearly increased two- to threefold by a 39 or 42°C heat shock or by treatment with α-deoxyglucose, tunicamycin, or brefeldin A (Fig. 4; Table 1). Thus, the presence of malfolded or improperly matured proteins apparently induces BiP expression in *P. carinii* much as it does in other organisms. In contrast, neither the calcium ionophore A23187 nor thapsigargin enhanced *Pcbip* mRNA levels under the conditions of these experiments (Fig. 4, lane 7; Table 1). Together, these results showed that *Pcbip* is regulated in patterns that are similar but not identical to those of previously characterized BiP genes in other organisms.

These analyses were limited by the lack of a robust continuous culture system for *P. carinii*, and therefore, we believe that the relative *Pcbip* stress response observed may have been underestimated. It is likely, if not probable, that the physical

◇, homology to HSE consensus sequences (5′-CNNGAANNTTCNNG-3′ [7, 45]); ○, homology to GC boxes (Sp1 transcription factor binding site); ●, homology to UPR in the *S. cerevisiae* Kar2 and mammalian BiP genes (5′-GGAANNGGNCAGCNTGNNGNNA-3′ [28, 36]). Several direct repeats in the 5′ flanking sequences of *Pcbip* are shown in bold, with arrows denoting their extent. (B) Alignment of PcBiP and PrBiP proteins. Amino acid identities are indicated by periods, and gaps are indicated by hyphens in the PrBiP sequence. The hydrophobic cores of the amino-terminal signal peptides are underlined. The −1 positions for probable signal peptidase cleavage sites are indicated in bold, and an inverted triangle shows the predicted cleavage sites in both proteins. The putative ER retention-recycling sequences at the carboxyl termini are also underlined and shown in bold.

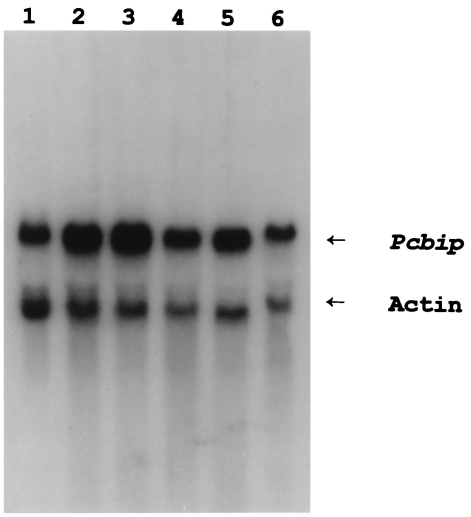

FIG. 4. Stress induction of *Pcbip* RNA in a transient culture. *P. c. carinii* short-term cultures were incubated briefly at 29°C and subjected to various stress conditions. Total RNA was isolated from each culture, and 20 μg was electrophoresed and blotted onto nylon filters as described in Materials and Methods. The blot was hybridized to 5′ end-labeled *Pcbip*-specific oligonucleotide probe 380Ar, which hybridized specifically to the ~2.5-kb *Pcbip* gene transcript. The blot was simultaneously hybridized to the *P. carinii*-specific actin gene probe PcAct, which hybridizes to the ~1.4-kb actin transcript, but not to rat actin mRNA, as a control for RNA levels. Hybridization to *Pcbip* mRNA was quantified with a Betascope radioanalytic imager (Betagen) and normalized to actin mRNA levels, and the fold induction was determined relative to *Pcbip* mRNA levels in untreated cultures (Table 1). Lanes: 1, control noninduced RNA; 2, heat shock for 10 min at 39°C; 3, heat shock for 30 min at 39°C; 4, 1 μg of tunicamycin per ml for 2 h; 5, 10 mM α-deoxyglucose for 2 h; 6, 10 μM A23187 (calcium ionophore) for 2 h. The locations of the ~2.5-kb *Pcbip* and ~1.4-kb actin gene transcripts are indicated.

insult associated with isolation of *P. carinii* from the host lung induces a stress response in the remaining viable organisms. Such a stress response was previously reported during isolation of rabbit type II pneumocytes (5). Thus, these experiments demonstrated, but may underestimate, the induction of *Pcbip* mRNA levels in response to stress.

***cis*-acting elements associated with *Pcbip* expression.** Promoter elements responsible for basal expression and induction of BiP genes have been identified in *S. cerevisiae* (28, 36) and some mammals (7, 45). Promoter elements responsible for constitutive BiP expression include GC-rich elements resembling Sp1 transcription factor binding sites localized within a few hundred base pairs of the transcription start point of the gene. Heat-inducible BiP genes in *S. cerevisiae*, *S. pombe*, and *K. lactis* also contain multiple heat shock elements (HSEs), which bind specific heat shock transcription factors and act as controlling elements for transcriptional regulation in response to heat or other forms of stress. These HSEs are loosely conserved, with a consensus sequence of 5′-CNNGAANNTTC NNG-3′ or contiguous arrays of the 5-bp unit NGAAN or NTTCN arranged in alternating orientations (reviewed in reference 33). Mammalian BiP genes, which are not heat inducible, lack functional HSEs (61). Finally, conditions leading to glucose starvation or to disruption of ER-golgi body transport, glycosylation, or intracellular Ca^{2+} levels mediate induction of BiP through a specific *cis*-acting DNA element referred to as unfolded protein response (UPR) element in *S. cerevisiae* (28, 36). This element exhibits a loose consensus sequence with an analogous domain in vertebrate and *Caenorhabditis elegans* BiP promoters (45).

Since regulation of *Pcbip* follows patterns observed for BiP genes in other organisms, we examined the 5′ flanking region of *Pcbip* for sequences resembling conserved regulatory elements associated with BiP gene expression. This examination revealed multiple TATA-like elements, including one ~25 bp upstream from the *Pcbip* transcription start point, and two GC-rich elements (Fig. 3), which together could form a basal transcription promoter. Candidate HSEs and a UPR-like element can also be identified in the 5′ flanking region of *Pcbip* (Fig. 3). The putative UPR-like element overlaps one of the potential GC-rich elements, similar to that described for the UPR and GC-rich elements in the *S. cerevisiae* BiP gene. The presence of these elements in the *Pcbip* 5′ flanking region is consistent with our empirical observations demonstrating stress response regulation of this gene, although verification of the functions of these putative regulatory elements is currently not possible because of the lack of a genetic system for *P. carinii*. Similar elements can also be identified in the *Prbip* gene sequence, but we have less confidence in their localization because we have been unable to map the transcription start point of this gene and the 5′ untranslated regions of *Pcbip* and *Prbip* are markedly divergent.

All introns in both *Pcbip* and *Prbip* conform to the consensus 5′ GYA splice donor sites and 3′ YAG splice acceptor sites of fungi (Fig. 3). The GC dinucleotide in the 5′ splice donor site of *Prbip* intron 2 is an unusual variant of the nearly ubiquitous GT (GU in RNA) dinucleotide but has been observed previously in fungal introns and introns in the *P. carinii* dihydrofolate reductase and thymidylate synthase genes (13, 16). Each BiP intron also displays a possible branch point consensus of YTRAT, similar to the *S. pombe* consensus CTRAY (35), within 20 bp of the 3′ splice acceptor sites (Fig. 3).

Molecular divergence between *Prbip* and *Pcbip*. Between the translation initiation and stop codons, *Pcbip* is a total of 29 bp (20 intronic bp and 9 coding bp) larger than *Prbip*. Pairwise alignments showed ~83% identity between the coding sequences of *Prbip* and *Pcbip* but only ~58% identity within the introns (Fig. 3). Thus, the introns in these two BiP genes are conserved in size and position but are not highly conserved in sequence. In contrast, the *P. carinii* BiP gene introns show no conservation in size or position when compared with introns in

TABLE 1. Induction of *Pcbip* expression in transient in vitro *P. carinii* culture

Isolates (no. of rats)	Control temp (°C)	Heat shock temp (°C)	Relative fold induction of *Pcbip* mRNA[a] treated with:						
			HS 10′	HS 30′	Tunc	α-d-glc	Bref-A	Thaps	A23187
2	29	39	2.0 ± 0.2	3.0 ± 0.3	1.8 ± 0.3	2.5 ± 0.2	ND[b]	ND	0.8 ± 0
3	35	42	1.3 ± 0.1	2.1 ± 0.3	1.8 ± 0.4	2.2 ± 0.2	1.8 ± 0.3	0.9 ± 0.3	ND

[a] Fold induction of *Pcbip* relative to untreated *P. carinii* (data not shown) and normalized to actin expression by using *P. carinii*-specific oligonucleotide probes p380Ar and PcAct, as described in Materials and Methods. HS 10′ and 30′, heat shock for 10 and 30 min, respectively. Tunc, 1 μM tunicamycin; α-d-glc, 10 mM α-deoxyglucose; Bref-A, 5 μM brefeldin A; Thaps, 2 μM thapsigargin; A23187, 10 μM A23187 (calcium ionophore).

[b] ND, not determined.

TABLE 2. Percent identity and percent similarity for selected BiP proteins

Organism	% Identity and % similarity[a]							
	P. c. carinii	*P. c. rattus*	*S. cerevisiae*	*K. actis*	*S. pombe*	Rat	Human	*T. cruzi*
P. c. rattus	94.8, 90.3							
S. cerevisiae	82.6, 69.4	82.0, 69.4						
K. actis	81.0, 66.8	80.0, 64.9	86.9, 77.6					
S. pombe	81.1, 68.6	81.3, 66.2	81.9, 68.1	80.8, 67.4				
Rat	80.5, 67.0	80.3, 65.4	81.7, 66.2	79.2, 63.3	80.6, 66.7			
Human	80.6, 66.8	79.8, 64.8	81.1, 65.9	79.2, 63.2	80.6, 66.2	98.8, 98.0		
T. cruzi	78.3, 59.9	77.1, 59.9	77.7, 60.8	75.9, 59.0	78.7, 60.7	79.3, 64.9	78.3, 63.9	
T. brucei	78.0, 60.5	76.8, 60.0	77.0, 59.8	74.5, 57.2	76.5, 59.6	78.6, 64.6	77.7, 63.9	95.1, 90.3

[a] The comparison was based on full protein alignments using the Smith and Waterman algorithm in the BESTFIT program of the GCG package with gap creation and extension penalties of 3 and 0.1, respectively. Alignments were visually confirmed to be full-length pairwise comparisons as described for those used for phylogenetic analysis. Number before comma, percent identity between the two proteins; number following comma, percent similarity between the two proteins.

the BiP genes of other organisms (data not shown). A convincing alignment of the 5′ flanking noncoding domains of *Prbip* and *Pcbip* was not possible, and we were therefore unable to verify, in *Prbip*, the presence of an intron corresponding to that in the 5′ untranslated region of *Pcbip*. The AT compositions of *Prbip* and *Pcbip* were ~61 and 63% for coding sequence, respectively, and ~62 and ~66% including intron and 5′ flanking sequence, respectively, thus conforming to the low-GC and high-AT codon bias previously reported for rat *P. carinii* genes (18). However, codon usage varied significantly between these genes since ~44% of the codons differ.

Apparent amino acid sequence identity between the PcBiP and PrBiP proteins is ~90% (Fig. 3B), which is greater than that between the *P. carinii* BiP genes and other *P. carinii* HSP70 homologs or HSP70 homologs of other organisms (51). However, the BiP homologs are more divergent than other proteins and RNAs that have been examined in both the prototype and variant strains of *P. carinii*; e.g., thymidylate synthase, β-tubulin, arom, 23S mitochondrial rRNA, and 18S nuclear rRNA show ~93 to 96% identity (10, 53). The homology observed between the *P. carinii* BiPs is considerably lower than the ~98% observed between rat and human BiPs and is comparable to the ~90% observed between the BiPs of the distantly related trypanosomes *Trypanosoma cruzi* and *Trypanosoma brucei* (Table 2). Together, these data show a surprisingly high degree of divergence between the normally highly conserved BiP gene homologs of these two *P. carinii* strains and are consistent with previous suggestions (9, 10, 52) that the prototype and variant rat *P. carinii* strains could be considered different species.

Phylogenetic analysis of PcBiP and PrBiP. BiP genes and proteins are ideal for phylogenetic analysis because of their high degree of primary sequence conservation. Thus, the PcBiP and PrBiP protein sequences were aligned with BiP sequences from representative members of each of the major eukaryotic kingdoms by use of the Pileup and Lineup programs in the GCG Sequence Analysis Package (data not shown). The aligned sequences extended from Gly-36 to Ala-603 of PcBiP (Gly-35 to Ala-602 of PrBiP), excluding the amino and carboxyl termini which could not be aligned unambiguously. An alignment of the cDNAs of each BiP homolog was also constructed on the basis of the protein alignment and corrected for codon placement in gaps (data not shown). The sequence of the prokaryotic HSP70 homolog *Escherichia coli* DnaK was included in the analysis to root the BiP phylogenetic trees.

Two methods of assessing phylogenetic distance were employed for tree construction. First, a protein parsimony approach using the PHYLIP (version 3.5) program PROTPARS with the global search option (17) generated a tree with the topology shown in Fig. 5A. More-favorable phylogenetic trees were sought by swapping and rearranging branches across small branch lengths. The initial alignment was bootstrapped 250 times with the program SEQBOOT, and a consensus tree was derived with the program CONSENSE to obtain bootstrap confidence values for clades found in the parsimony tree. Second, a distance matrix approach was performed with the DNA alignment by use of the maximum likelihood distance algorithm in DNADIST. The alignment was weighted to consider only the first two bases of each codon to reduce homoplastic noise associated with the third base position, attributable to large evolutionary distance and the strong codon bias of several of the organisms, including *Giardia lamblia*, *P. falciparum*, and *P. carinii*. The alignment was bootstrapped 250 times, the maximum likelihood distance matrix data were collected, and a consensus neighbor-joining (47) tree was generated (Fig. 5B).

The trees generated by the protein parsimony and DNA distance approaches are similar. Both methods group species belonging to the metazoa and higher fungi as monophyletic taxa, with bootstrap confidence supporting these groups at or near 100%. In addition, *P. c. carinii* and *P. c. rattus* grouped as terminal ancestors and with the ascomycetes *S. pombe*, *K. lactis*, and *S. cerevisiae*, as a monophyletic group distinct from other groups of eukaryotes. The first genetic evidence for classification of *P. carinii* with the fungi was based on the sequence of the 18S rRNA (14, 56). Wakefield et al. (60) analyzed mitochondrial rRNA to attempt a more definitive placement of *P. carinii* within the fungi and proposed similarity with the ustomycetous red yeasts, although a sequence-based phylogenetic analysis was not shown. More recently, analysis of the α-actin gene also supported classification of *P. carinii* with the fungi (19). Our analysis of the *P. carinii* BiP homologs, which are large, highly conserved proteins with many phylogenetically informative sites, strongly supports inclusion of *P. c. carinii* and *P. c. rattus* among the higher fungi, as represented here by three ascomycetes. However, relative placement of the *P. carinii* strains within this group is currently precluded by the paucity of available fungal BiP sequences.

Members of the Protoctista displayed a polyphyletic origin in these analyses. The oomycete *Phytophthora cinnamomi* branched well before the fungi, supporting early divergence of oomycetes prior to speciation of the fungi proper (1, 27). Not surprisingly, a unique rooting point could not be determined for the apicomplexan malarial parasite *P. falciparum*, which branched inconsistently at the base of fungal and plant clades in trees generated by both methods. Apicomplexa share apparent ancestry with both dinoflagellates and ciliates (20), are proposed to have arisen via an endosymbiotic pathway involving an ancestral eukaryote and a rhodophytic alga (63), and

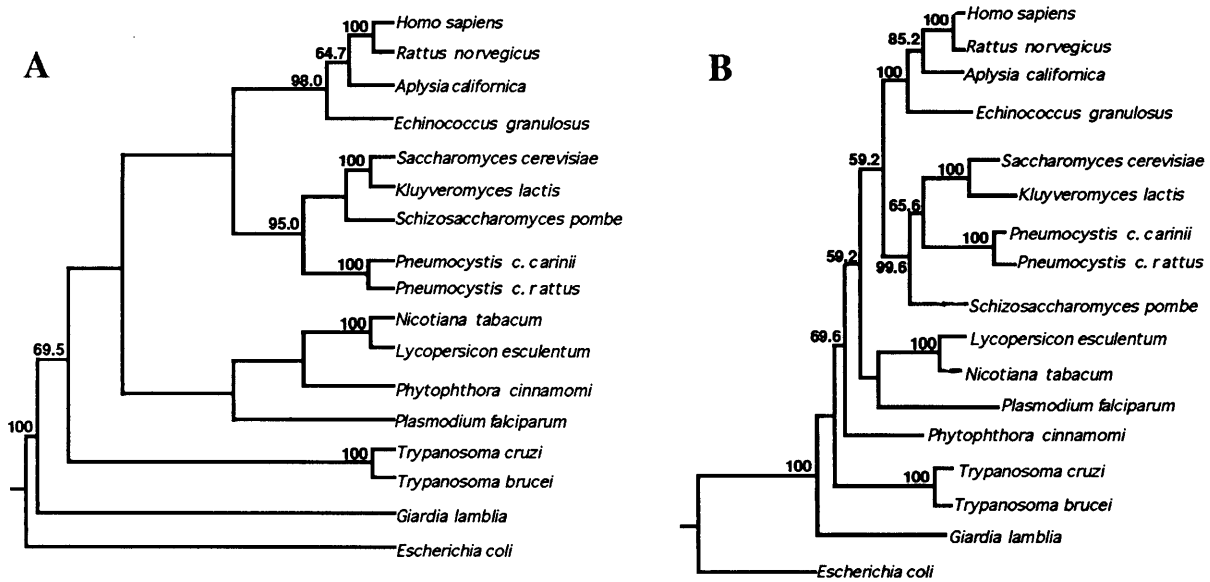

FIG. 5. Phylogenetic analysis of PcBiP and PrBiP. (A) Protein parsimony tree derived from alignment of BiP proteins by use of the PHYLIP version 3.5c programs PROTPARS, SEQBOOT, and CONSENSUS. Branch lengths are not significant. (B) Phylogenetic tree generated from aligned BiP DNA sequences by using maximum likelihood matrix analysis in the DNADIST program and the neighbor-joining method for tree construction, with branch lengths reestimated by use of the FITCH program. Bootstrap values at the nodes of each tree represent confidence intervals supporting the exclusive placement of all species to the right of each node. Only values greater than 50 per 100 trees are shown, on the basis of a sequence data set bootstrapped 250 times. Trees were rooted by inclusion of the *E. coli* DnaK protein or gene in the respective alignments as described in the text. The genes (and their GenBank accession numbers) used in this analysis were from the following organisms: *G. lamblia* (U04875); *T. brucei* (L14477); *T. cruzi* (L23420); *P. falciparum* (L02822 and L02823); *Phytophthora cinnamomi*, an oomycete (X75673); *Homo sapiens* (M19645); *Rattus norvegicus* (M14050); *Aplysia californica*, sea hare (Z15041); *Echinococcus granulosis*, tapeworm (M63605); *Nicotiana tabacum*, tobacco (X60057/S43495); *Lycopersicon esculentum*, tomato (L08830); *S. cerevisiae* (M25394); *K. lactis* (X54709); *S. pombe* (X64416); *P. c. carinii* prototype strain (L46790); *P. c. rattus* variant strain (U40994); and *E. coli* DnaK (K01298).

contain residual plastid genomes. Like BiP, the nuclear-encoded *P. falciparum* enolase also resembles plant enolases more closely than those of other eukaryotes (44), perhaps suggesting a major influence of the ancestral plastid genome on the nuclear genome. However, a large mutational distance separates *Plasmodium* spp. from other eukaryotes, and these organisms have been subjected to accelerated rates of evolutionary change (20), a property known to confound the construction of evolutionary trees. Of the lower protists, the trypanosomes were monophyletic, as was the primitive mitochondrion-lacking eukaryote *G. lamblia.*

Previous phylogenetic analyses with members of the HSP70 gene family have included a few BiP sequences (4, 22, 39). Despite small branch lengths and although not supported at a high level of confidence by bootstrap methods, we infer from the BiP trees presented here a more recent common ancestry for animals and fungi than for either one with plants, consistent with proposals of others (38, 59) in this long-standing controversy. Our results are in contrast to a previous parsimony analysis using members of the HSP70 family of proteins (22), which concluded that the BiP homolog of *S. cerevisiae* is deep branching among the eukaryotes. The consensus tree in the latter analysis did not support this topology, however, and more importantly, *S. cerevisiae* was the only fungus examined. In contrast, several members of the ascomycetes and related fungi have been used herein, permitting a clearer resolution of the evolutionary lineage of higher fungi.

ACKNOWLEDGMENTS

We thank Tom Reynolds and the MCV-VCU Nucleic Acids Core Facility for oligonucleotide synthesis and automated sequencing.

This work was supported by grants from the NIH, the Jeffress Memorial Trust, and the A. D. Williams Foundation.

REFERENCES

1. **Auwera, G. V., S. Chapelle, and R. D. Wachter.** 1994. Structure of the large ribosomal subunit RNA of *Phytophthora megasperma*, and phylogeny of the oomycetes. FEBS Lett. **338:**133–136.
2. **Bartlett, M. S., and J. W. Smith.** 1991. *Pneumocystis carinii*, an opportunist in immunocompromised patients. Clin. Microbiol. Rev. **4:**137–149.
3. **Bauer, N. L., J. R. Paulsrud, M. S. Bartlett, J. W. Smith, and C. E. Wilde.** 1993. *Pneumocystis carinii* organisms obtained from rats, ferrets, and mice are antigenically different. Infect. Immun. **61:**1315–1319.
4. **Boorstein, W. R., T. Ziegelhoffer, and E. A. Craig.** 1994. Molecular evolution of the HSP70 multigene family. J. Mol. Evol. **38:**1–17.
5. **Brandes, M. E., and J. N. Finkelstein.** 1989. Induction of the stress response by isolation of rabbit type II pneumocytes. Exp. Lung Res. **15:**93–111.
6. **Brodsky, J. L., S. Hamamoto, D. Feldheim, and R. Schekman.** 1993. Reconstitution of protein translocation from solubilized yeast membranes reveals topologically distinct roles for BiP and cytosolic Hsc70. J. Cell Biol. **120:**95–102.
7. **Chang, S. C., A. E. Erwin, and A. S. Lee.** 1989. Glucose-regulated protein (GRP94 and GRP78) genes share common regulatory domains and are coordinately regulated by common *trans*-acting factors. Mol. Cell. Biol. **9:**2153–2162.
8. **Church, G., and W. Gilbert.** 1984. Genomic sequencing. Proc. Natl. Acad. Sci. USA **81:**1991–1995.
9. **Cushion, M. T., M. Kaselis, S. L. Stringer, and J. R. Stringer.** 1993. Genetic stability and diversity of *Pneumocystis carinii* infecting rat colonies. Infect. Immun. **61:**4801–4813.
10. **Cushion, M. T., J. Zhang, M. Kaselis, D. Giuntoli, S. Stringer, and J. R. Stringer.** 1993. Evidence for two genetic variants of *Pneumocystis carinii* coinfecting laboratory rats. J. Clin. Microbiol. **31:**1217–1223.
11. **De Stefano, J. A., M. T. Cushion, V. Puvanesarajah, and P. D. Walzer.** 1990. Analysis of *Pneumocystis carinii* cyst wall. II. Sugar composition. J. Protozool. **37:**436–441.
12. **De Stefano, J. A., M. T. Cushion, R. G. Sleight, and P. D. Walzer.** 1990. Analysis of *Pneumocystis carinii* cyst wall. I. Evidence for an outer surface membrane. J. Protozool. **37:**428–435.
13. **Edman, J. C., U. Edman, M. Cao, B. Lundgren, J. A. Kovacs, and D. V. Santi.** 1989. Isolation and expression of the *Pneumocystis carinii* dihydrofolate reductase gene. Proc. Natl. Acad. Sci. USA **86:**8625–8629.
14. **Edman, J. C., J. A. Kovacs, H. Masur, D. V. Santi, H. J. Elwood, and M. L. Sogin.** 1988. Ribosomal RNA sequence shows *Pneumocystis carinii* to be a member of the fungi. Nature (London) **334:**519–522.

15. **Edman, J. C., and M. L. Sogin.** 1994. Molecular phylogeny of *Pneumocystis carinii*, p. 91–105. *In* P. D. Walzer (ed). *Pneumocystis carinii* pneumonia, 2nd ed. Marcel Dekker, Inc., New York.
16. **Edman, U., J. C. Edman, B. Lundgren, and D. V. Santi.** 1989. Isolation and expression of the *Pneumocystis carinii* thymidylate synthase gene. Proc. Natl. Acad. Sci. USA **86:**6503–6507.
17. **Felsenstein, J.** 1989. PHYLIP—phylogeny inference package (version 3.2). Cladistics **5:**164–166.
18. **Fletcher, L. D., L. C. Berger, S. A. Peel, R. S. Baric, R. R. Tidwell, and C. C. Dykstra.** 1993. Isolation and identification of six *Pneumocystis carinii* genes utilizing codon bias. Gene **129:**167–174.
19. **Fletcher, L. D., J. M. McDowell, R. R. Tidwell, R. B. Meagher, and C. C. Dykstra.** 1994. Structure, expression and phylogenetic analysis of the gene encoding actin I in *Pneumocystis carinii*. Genetics **137:**743–750.
20. **Gajadhar, A. A., W. C. Marquardt, R. Hall, J. Gunderson, E. V. Ariztia-Carmona, and M. L. Sogin.** 1991. Ribosomal RNA sequences of *Sarcocystis muris*, *Theileria annulata*, and *Crypthecodinium cohnii* reveal evolutionary relationships among apicomplexans, dinoflagellates and ciliates. Mol. Biochem. Parasitol. **45:**147–154.
21. **Gething, M., and J. Sambrook.** 1992. Protein folding in the cell. Nature (London) **355:**33–45.
22. **Gupta, R. S., K. Aitken, M. Falah, and B. Singh.** 1994. Cloning of the *Giardia lamblia* heat shock protein HSP70 homologs: implications regarding origin of eukaryotic cells and of endoplasmic reticulum. Proc. Natl. Acad. Sci. USA **91:**2895–2899.
23. **Gupta, R. S., and B. Golding.** 1993. Evolution of HSP70 gene and its implications regarding relationships between archaebacteria, eubacteria, and eucaryotes. J. Mol. Evol. **37:**573–582.
24. **Haas, I. G.** 1994. BiP (GRP78), an essential hsp70 resident protein in the endoplasmic reticulum. Experientia **50:**1012–1020.
25. **Haidaris, P. J., T. W. Wright, F. Gigliotti, and C. G. Haidaris.** 1992. Expression and characterization of a cDNA clone encoding an immunodominant surface glycoprotein of *Pneumocystis carinii*. J. Infect. Dis. **166:**1113–1123.
26. **Hughes, A. L.** 1993. Nonlinear relationships among evolutionary rates identify regions of functional divergence in heat-shock protein 70 genes. Mol. Biol. Evol. **10:**243–255.
27. **Karlovsky, P., and H. H. Prell.** 1991. The TRP1 gene of *Phytophthora parasitica* encoding indole-3 glycerolphosphate synthase-*N*-(5′-phosphoribosyl)anthranilate isomerase: structure and evolutionary distance from homologous fungal genes. Gene **109:**161–165.
28. **Kohno, K., K. Normington, J. Sambrook, M. Gething, and K. Mori.** 1993. The promoter region of the yeast KAR2 (BiP) gene contains a regulatory domain that responds to the presence of unfolded proteins in the endoplasmic reticulum. Mol. Cell. Biol. **13:**877–890.
29. **Kovacs, J. A., F. Powell, J. C. Edman, B. Lundgren, A. Martinez, B. Drew, and C. W. Angus.** 1993. Multiple genes encode the major surface glycoprotein of *Pneumocystis carinii*. J. Biol. Chem. **268:**6034–6040.
30. **Kozutsumi, Y., M. Segal, K. Normington, M. J. Gething, and J. Sambrook.** 1988. The presence of unfolded proteins in the endoplasmic reticulum signals the induction of glucose-regulated proteins. Nature (London) **332:**462–464.
31. **Lee, A. S.** 1987. Coordinated regulation of a set of genes by glucose and calcium ionophores in mammalian cells. Trends Biochem. Sci. **12:**20–23.
32. **Lewis, M. J., and H. R. Pelham.** 1990. A human homologue of the yeast HDEL receptor. Nature (London) **348:**162–163.
33. **Lis, J. T., H. Xiao, and O. Perisic.** 1989. A structural unit of heat shock regulatory regions, p. 73–82. *In* M. L. Pardue, J. R. Feramisco, and S. Lindquist (ed.), Stress induced proteins. Alan R. Liss, Inc., New York.
34. **Liu, E., J. Ou, and A. S. Lee.** 1992. Brefeldin A as a regulator of grp78 gene expression in mammalian cells. J. Biol. Chem. **267:**7128–7133.
35. **Mertins, P., and D. Gallwitz.** 1987. Nuclear pre-mRNA splicing in the fission yeast *Schizosaccharomyces pombe* strictly requires an intron-contained, conserved sequence element. EMBO J. **11:**2583–2593.
36. **Mori, K., A. Sant, K. Kohno, K. Normington, M. Gething, and J. F. Sambrook.** 1992. A 22 bp *cis*-acting element is necessary and sufficient for the induction of the yeast *KAR2* (BiP) gene by unfolded proteins. EMBO J. **11:**2583–2593.
37. **Munro, S., and H. R. B. Pelham.** 1987. A C-terminal signal prevents secretion of luminal ER proteins. Cell **48:**899–907.
38. **Nikoh, N., N. Hayase, N. Iwabe, K. Kuma, and T. Miyata.** 1994. Phylogenetic relationship of the kingdoms Animalia, Plantae, and Fungi, inferred from 23 different protein species. Mol. Biol. Evol. **11:**762–768.
39. **Normington, K., K. Kohno, Y. Kozutsumi, M. Gething, and J. Sambrook.** 1989. *S. cerevisiae* encodes an essential protein homologous in sequence and function to mammalian BiP. Cell **57:**1223–1236.
40. **Paulsrud, J. R., S. F. Queener, M. S. Bartlett, and J. W. Smith.** 1993. Total cellular fatty acid composition of cultured *Pneumocystis carinii*. J. Clin. Microbiol. **31:**1899–1902.
41. **Peterson, M., and R. Tjian.** 1993. Cross-species polymerase chain reaction: cloning of TATA box binding proteins. Methods Enzymol. **218:**493–507.
42. **Pidoux, A. L., and J. Armstrong.** 1992. Analysis of the BiP gene and identification of an ER retention signal in *Schizosaccharomyces pombe*. EMBO J. **11:**1583–1591.
43. **Price, B. D., L. A. Mannheim-Rodman, and S. K. Calderwood.** 1992. Brefeldin A, thapsigargin, and A1F stimulate the accumulation of GRP78 mRNA in a cycloheximide dependent manner, whilst induction by hypoxia is independent of protein synthesis. J. Cell Physiol. **152:**545–552.
44. **Read, M., K. E. Hicks, P. F. G. Sims, and J. E. Hyde.** 1994. Molecular characterisation of the enolase gene from the human malarial parasite *Plasmodium falciparum*. Eur. J. Biochem. **220:**513–520.
45. **Resendez, E., S. K. Wooden, and A. S. Lee.** 1988. Identification of highly conserved regulatory domains and protein-binding sites in the promoters of the rat and human genes encoding the stress-inducible 78-kilodalton glucose-regulated protein. Mol. Cell. Biol. **8:**4579–4584.
46. **Rose, M. D., L. M. Misra, and J. P. Vogel.** 1989. *KAR2*, a karyogamy gene, is the yeast homolog of the mammalian BiP/GRP78 gene. Cell **57:**1211–1221.
47. **Saitou, N., and M. Nei.** 1995. The neighbor-joining method: a new method for reconstructing phylogenetic trees. Mol. Biol. Evol. **3:**282–284.
48. **Sambrook, J., E. F. Fritsch, and T. Maniatis.** 1989. Molecular cloning: a laboratory manual. Cold Spring Harbor Laboratory Press, Cold Spring Harbor, N.Y.
49. **Semenza, J. C., and H. R. Pelham.** 1992. Changing the specificity of the sorting receptor for luminal endoplasmic reticulum proteins. J. Mol. Biol. **224:**1–5.
50. **Sinclair, K., A. E. Wakefield, S. Banerji, and J. M. Hopkin.** 1991. *Pneumocystis carinii* organisms derived from rat and human hosts are genetically distinct. Mol. Biochem. Parasitol. **45:**183–184.
51. **Stedman, T. T., D. R. Butler, and G. A. Buck.** Unpublished data.
52. **Stringer, J. R.** 1993. The identity of *Pneumocystis carinii*: not a single protozoan, but a diverse group of exotic fungi. Infect. Agents Dis. **2:**109–117.
53. **Stringer, J. R., et al. (The** *Pneumocystis* Workshop). 1994. Revised nomenclature for *Pneumocystis carinii*. J. Eukaryot. Microbiol. **41:**121S–122S.
54. **Stringer, J. R., J. C. Edman, M. T. Cushion, F. F. Richards, and J. Watanabe.** 1992. The fungal nature of *Pneumocystis*. J. Med. Vet. Mycol. **30**(Suppl. 1)**:**271–278.
55. **Stringer, J. R., S. L. Stringer, J. Zhang, R. Baughman, A. G. Smulian, and M. T. Cushion.** 1993. Molecular genetic distinction of *Pneumocystis carinii* from rats and humans. J. Eukaryot. Microbiol. **40:**733–741.
56. **Stringer, S. L., J. R. Stringer, M. A. Blase, P. D. Walzer, and M. T. Cushion.** 1989. *Pneumocystis carinii*: sequence from ribosomal RNA implies a close relationship with fungi. Exp. Parasitol. **68:**450–461.
57. **Vogel, J. P., J. N. Lee, D. R. Kirsch, M. D. Rose, and E. S. Sztul.** 1993. Brefeldin A causes a defect in secretion in *Saccharomyces cerevisiae*. J. Biol. Chem. **268:**3040–3043.
58. **Wada, M., K. Kitada, M. Saito, K. Egawa, and Y. Nakamura.** 1993. cDNA sequence diversity and genomic clusters of major surface glycoprotein genes of *Pneumocystis carinii*. J. Infect. Dis. **168:**979–985.
59. **Wainright, P. O., G. Hinkle, M. L. Sogin, and S. K. Stickel.** 1993. Monophyletic origins of the metazoa: an evolutionary link with fungi. Science **260:**340–342.
60. **Wakefield, A. E., S. E. Peters, S. Banerji, P. D. Bridge, G. S. Hall, D. L. Hawksworth, L. A. Guiver, A. G. Allen, and J. M. Hopkin.** 1992. *Pneumocystis carinii* shows DNA homology with the ustomycetous red yeast fungi. Mol. Microbiol. **6:**1903–1911.
61. **Watowich, S. S., and R. I. Morimoto.** 1988. Complex regulation of heat shock and glucose responsive genes in human cells. Mol. Cell. Biol. **8:**393–405.
62. **Williams, D. J., J. A. Radding, A. Dell, K. Khoo, M. E. Rogers, F. F. Richards, and M. Y. K. Armstrong.** 1991. Glucan synthesis in *Pneumocystis carinii*. J. Protozool. **38:**427–437.
63. **Williamson, D. H., M. J. Gardner, P. Preiser, D. J. Moore, K. Rangachari, and R. J. M. Wilson.** 1994. The evolutionary origin of the 35 kb circular DNA of *Plasmodium falciparum*: new evidence supports a possible rhodophyte ancestry. Mol. Gen. Genet. **243:**249–252.
64. **Yoganathan, T., H. Lin, and G. A. Buck.** 1989. An electrophoretic karyotype and assignment of ribosomal genes to resolved chromosomes of *Pneumocystis carinii*. Mol. Microbiol. **3:**1473–1480.

Editor: D. H. Howard